The interlaminar fracture behaviour and toughening mechanisms of new carbon fibre-reinforced bismaleimide composites

X.J. Xian*
Institute of Mechanics, Chinese Academy of Sciences, Beijing, People's Republic of China

and C.L Choy
Department of Applied Physics, Hong Kong Polytechnic, Hung Hom, Kowloon, Hong Kong
(Revised 16 March 1993)

The interlaminar fracture behaviour of carbon fibre-reinforced bismaleimide (BMI) composites prepared by using a new modified BMI matrix has been investigated by various methods. Laminates of three typical stacking sequences were evaluated. Double cantilever beam, end-notch flexure and edge-delamination tension tests were conducted under conventional conditions and in a scanning electron microscope. The strain energy release rates in Mode I and Mode II, G_{Ic} and G_{IIc}, as well as the total strain energy release rate, G_{mc}, have been determined and found to be higher than those for laminates with an epoxy matrix. Dynamic delamination propagation was also studied. The toughening mechanisms are discussed.

(Keywords: bismaleimide matrix composites; interlaminar fracture behaviour; toughening mechanisms; Mode I; Mode II; mixed mode)

INTRODUCTION

The failure modes of composite laminates mainly include matrix cracking, delamination and fibre breakage. However, delamination (interlaminar debonding) is the most important process. Even if there are cracks in the matrix, the laminate can still sustain loads. Fibres are the main load-bearing component, but break mostly in the final stage. Nevertheless, from the initiation of damage to failure of the laminate, delamination propagation is the major factor. Thus, delamination would limit the application and service life of composite structures. Delamination can result from impact, compressive, transverse tensile and shear stresses. In recent years, some attention has been paid to the analysis and control of delamination and to the determination of interlaminar fracture toughness. The critical interlaminar fracture toughness, G_c, is an important parameter characterizing the toughness and delamination resistance of a composite and is commonly used in damage and fracture calculations. There is a significant number of studies[1-4] on G_c of unidirectional composites, but very little work[5,6] has been reported on the interlaminar fracture toughness of multidirectional laminates, which is even more complex. It is thus important to find suitable methods to determine the interlaminar fracture toughness, to investigate delamination propagation and to analyse the toughening mechanisms on a microscopic basis.

Epoxy is the commonly used matrix in composites but it is limited by its low fracture toughness, low delamination resistance and poor performance in hot/wet environments. Epoxy can be toughened by the addition of rubber but its thermal resistance is significantly reduced. In recent years, bismaleimide resins with good thermal properties have been developed[7,8]. However, such materials are limited by their brittleness and processing difficulties. A new modified bismaleimide (MBMI) has been recently produced[9]. This material possesses good toughness, higher thermal resistance and good processability.

This paper is concerned with the interlaminar fracture characteristics of a carbon/bismaleimide (BMI) composite prepared using this new modified BMI matrix. The interlaminar fracture toughness and delamination propagation of laminates with three typical lay-ups were evaluated. Double cantilever beam (DCB for Mode I G_{Ic}) and end-notch flexure (ENF for Mode II G_{IIc}) tests were conducted under conventional conditions and in a scanning electron microscope (SEM). We have also used the edge-delamination tension (EDT)[10] method to measure the mixed-mode interlaminar fracture toughness G_{mc}. Delamination occurrence and propagation in laminates have been observed in real time by scanning electron microscopy.

SPECIMEN PREPARATION AND EXPERIMENTAL METHODS

The test specimens were machined from panels made of Toray T300 carbon fibres in an MBMI matrix. The fibre volume fraction, V_f, was 60–61%. The matrix was a commercially available bismaleimide modified by com-

*To whom correspondence should be addressed

0010-4361/95/01/0033-07

pounding with poly(ether sulfone) (PES). MBMI was dissolved in a low boiling point solvent. T300 carbon fibre unidirectional prepreg was made by the solvent method. The composites were cured at 177°C in an autoclave under a pressure of 5 bar for 2 h, then moved into an oven for post-curing at 120°C for 5 h. The thickness of each ply was 0.11 mm. The nominal thicknesses of the laminates for DCB and ENF tests were 3 mm. The three types of specimen examined by the DCB and ENF techniques had the following stacking sequences: $[0]_{26}$, $[0/90]_{6s}$ and $[\pm 45]_{6s}$. A precrack was formed prior to curing by inserting a 12 μm thick Teflon film in the midplane on one edge of the laminates. The initial crack length, a_0, was 20 mm. All the specimens were examined by X-ray and ultrasonic C-scanning for quality control.

The critical interlaminar fracture toughness in the separation mode (Mode I), G_{Ic}, was determined by the DCB method. A special holder was designed so that the cantilevers on the specimen were held by the grips of an Instron 1195 testing machine and a load was applied. The specimen was 24 mm wide and 200 mm long. The interlaminar fracture toughness in the shear mode (Mode II), G_{IIc}, was measured by the ENF method, which was essentially a three-point flexure loading measurement. The specimen was 20 mm wide and 60 mm long. In both tests, the load (P) *versus* displacement (δ) curves were traced on a chart recorder. For Mode I, δ was the opening displacement while for Mode II, δ was the bending displacement of the middle point of the beam. When the load reached a critical value P_c (also denoted by P_1) the precrack (a_0) grew and the increase in crack length Δa was measured. Then the load was reduced to zero. This procedure was repeated many times. Each crack extension was measured by a travelling microscope and photographs were taken using a Wild M3 long focal distance microscope. From the above data, G_{Ic} and G_{IIc} can be calculated. Small DCB (50 × 6 × 2 mm^3) and ENF (20 × 6 × 2 mm^3) T300/MBMI specimens were also tested in an S570 Hitachi SEM. For comparison, T300/epoxy specimens were also studied. The dynamic propagation of interlaminar delamination and interface damage were observed and recorded *in situ*.

Interlaminar fracture can occur in Mode I (interlaminar tension) or Mode II (interlaminar shear). These modes are usually mixed in practice, hence the term 'mixed-mode fracture'. The critical interlaminar fracture toughness in the mixed mode, G_{mc}, was determined by the EDT method. By stress analysis, a laminate with $[\pm 30_2/90/\overline{90}]_s$ lay-up was found to have very high free-edge interlaminar stresses[10] at the $-30/90$ interface. The specimen studied by this method was 254 mm long, 38 mm wide and 1.36 mm thick. For each lay-up and fracture mode five specimens were tested.

DETERMINATION OF INTERLAMINAR FRACTURE TOUGHNESS

The interlaminar fracture toughness is characterized by the critical strain energy release rate, G_c. The compliance method, area method and linear elastic fracture mechanics (LEFM) polynomial form were used for the calculation of G_c.

Mode I

Compliance method. G_c is given by[11]:

$$G_{Ic} = \frac{P_c^2 a^2}{bEI} \tag{1}$$

where b, E and I are the width, elastic modulus and moment of inertia of the specimen, respectively.

Area method. By definition,

$$G_c = -\frac{1}{b}\left(\frac{dU}{da}\right) \tag{2}$$

where U is the total energy in the body. When the load–displacement curves for the cracked specimens exhibit a linear elastic response, the change in U due to crack extension from a to $(a + \Delta a)$ is simply the area between the loading and unloading curves. Thus G_{Ic} is given by[11]:

$$G_{Ic} = \frac{1}{2b(\Delta a)}[P_1\delta_2 - P_2\delta_1) \tag{3}$$

LEFM polynomial form. The stress intensity factor (K_{Ic}) and strain energy release rate (G_{Ic}) can be calculated from the following expressions[6]:

$$K_{Ic} = \frac{4P_c}{bh^{3/2}}(3a^2 + 3.84\,ha + 1.22\,h^2)^{1/2} \tag{3}$$

$$G_{Ic} = \frac{K_{Ic}^2}{E} + \frac{P_c^2}{bS'} \tag{4}$$

where h is one-half of the specimen thickness, E is the shear modulus, and $S' = 5/6 \times$ cross-sectional area of the beam.

Mode II

Compliance method. G_{IIc} is given by[12]:

$$G_{IIc} = \frac{9a^2P_c^2C}{2b(2L^3 + 3a^3)} \tag{5}$$

where C is the specimen compliance and L is the span between the central loading pin and the outer support pins.

LEFM polynomial form. K_{IIc} and G_{IIc} are given by[6]:

$$K_{IIc} = \frac{3P_c a}{2bh^{3/2}} \tag{6}$$

$$G_{IIc} = \frac{K_{IIc}}{E} \tag{7}$$

The above results are obtained from linear analyses. It has been shown[13] that for the worst case (large crack length at critical load), the difference in the computed compliances from linear and non-linear analyses is only 5%.

Mixed mode

For $[\pm 30_2/90/\overline{90}]_s$ laminates, a marked change in the slope of the load *versus* deformation curve occurs at the onset of edge delamination. The strain at the onset of delamination is substituted into a closed-form equation for the strain energy release rate to obtain the critical value G_{mc} for edge delamination. The fracture mechanics

Table 1 Interlaminar fracture toughness of T300/MBMI laminates

Specimen lay-up	G_{Ic} (J m $^{-2}$)				G_{IIc} (J m $^{-2}$)		
	Compliance method	Area method	Polynomial form	Average	Compliance method	Polynomial form	Average
$[0]_{26}$	307	305	356	323	739	814	777
$[0/90]_{6s}$	171	153	189	171	414	460	437
$[\pm 45]_{6s}$	153	110	132	132	410	554	482

analysis is based upon the axial stiffness loss of the laminate as a result of the growth of delamination. Under fixed grip condition, the strain energy release rate is[10]:

$$G_c = \epsilon_c^2 t(E_x - E^*)/2 \quad (8)$$

where ϵ_c is the axial tensile strain at delamination onset, t is the specimen thickness, E_x is the axial modulus of the specimen before delamination and E^* is the elastic modulus of the specimen after delamination.

The experimental results (values of G_c at initiation) are shown in *Table 1*. The agreement between the G_{Ic} and G_{IIc} values obtained from different methods is reasonable. For the $[\pm 45]_{6s}$ specimens, the delamination propagation paths are irregular, thereby leading to more scattered values. The average G_{Ic} and G_{IIc} values for the T300/MBMI $[0]_{26}$ specimen are 323 and 777 J m^{-2} respectively, which are substantially higher than those of T300/epoxy laminates ($G_{Ic} \approx 100$ and 200 J m^{-2} for 5208 and 914 epoxy[4] and $G_{IIc} = 456$ and 518 J m^{-2} for 3501-6 and 914 epoxy[14]). This implies that the modified BMI matrix has a considerable toughening effect. The G_{Ic} and G_{IIc} values of the $[0]_{26}$ laminates are higher than those of the $[0/90]_{6s}$ and $[\pm 45]_{6s}$ laminates. This arises because there is fibre bridging in the $[0]_{26}$ laminates.

An average mixed-mode G_{mc} value of 295 J m^{-2} was obtained for the T300 carbon fibre-reinforced MBMI composite. This is about 70% higher than that of T300 fibre-reinforced epoxy[14], indicating that the use of a modified BMI matrix leads to an improvement in the delamination resistance.

CRACK PROPAGATION AND DELAMINATION

Mode I interlaminar crack growth in the 0° laminates is along the precrack plane in the 0° direction (*Figure 1*). The critical delamination propagation is shown more clearly in the high magnification picture (*Figure 2*). Fibres are pulled out behind the crack tip. A few fibres are bridging the crack and are subsequently broken by bending.

The interlaminar crack growth in the multidirectional laminates involves splitting of the crack tip into a primary crack and a secondary crack, with the latter branching off the precrack planes. For the $[\pm 45]_{6s}$ laminate, the crack grows mainly along the horizontal precrack, then turns 45° through the thickness of a 45° ply (*Figure 3*). For the $[0/90]_{6s}$ laminate, the main crack grows along the precrack plane first, then one subcrack branches through the thickness of a 90° ply (*Figure 4*). After that, for both the $[0/90]_{6s}$ and $[\pm 45]_{6s}$ laminates, the crack propagates along the interface between two plies.

In Mode II, the crack pattern of the unidirectional

Figure 1 Mode I interlaminar crack propagation in T300/MBMI $[0]_{26}$ specimen. The crack propagation direction is upwards

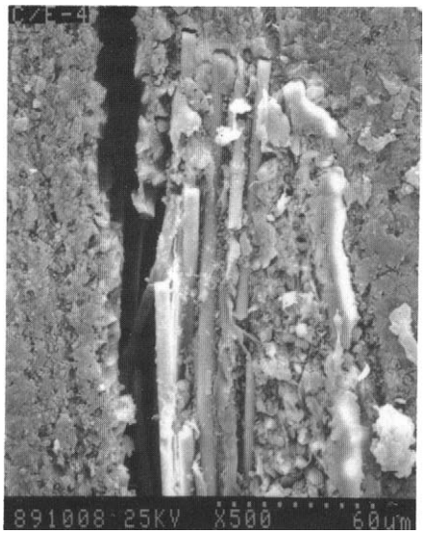

Figure 2 Mode I critical delamination propagation and fibre bridging in T300/MBMI $[0]_{26}$ specimen

specimen was found to be essentially the same as in Mode I, and the interference between cracks was minor. However, the damage zones in multidirectional specimens are larger due to the larger load-bearing area. Take the $[0/90]_{6s}$ cross-plied specimen as an example. Under critical flexure loading P_c, the main crack grows in the precrack plane. With an increase in load, subcracks

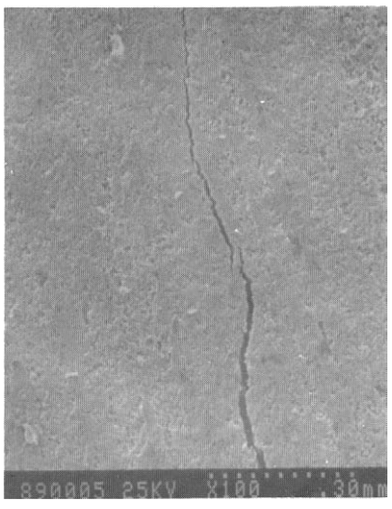

Figure 3 Mode I interlaminar crack propagation in T300/MBMI $[\pm 45]_{6s}$ specimen. The crack propagation direction is upwards

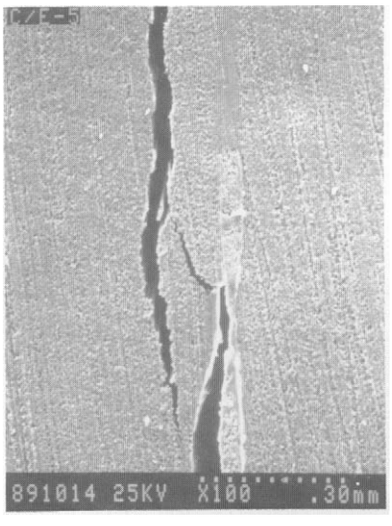

Figure 4 Mode I main crack and subcrack in T300/MBMI $[0/90]_{6s}$ specimen

occur and propagate. Transverse cracks through the 90° ply and delamination at the 0/90 interfaces were observed in the neighbouring plies (*Figure 5*). There is good adhesion between the fibres and the matrix.

Thus, the mechanisms of interlaminar crack growth in unidirectional laminates involve crack-tip splitting, fibre pull-out behind the crack tip and some fibre bridging as well as interface debonding. For multidirectional composites, delamination is still the dominant cracking mechanism. After the main crack has grown in the precrack plane, subcracks occur in the 90° or 45° ply but they play virtually no role in the failure process.

Figure 6 shows the onset of edge delamination in three $[\pm 30_2/90/\overline{90}]_s$ specimens. Delamination occurs mainly at the $-30/90$ interface at which there is a high free-edge interlaminar stress. *Figure 7* and *Figure 8* show the delamination at high magnification.

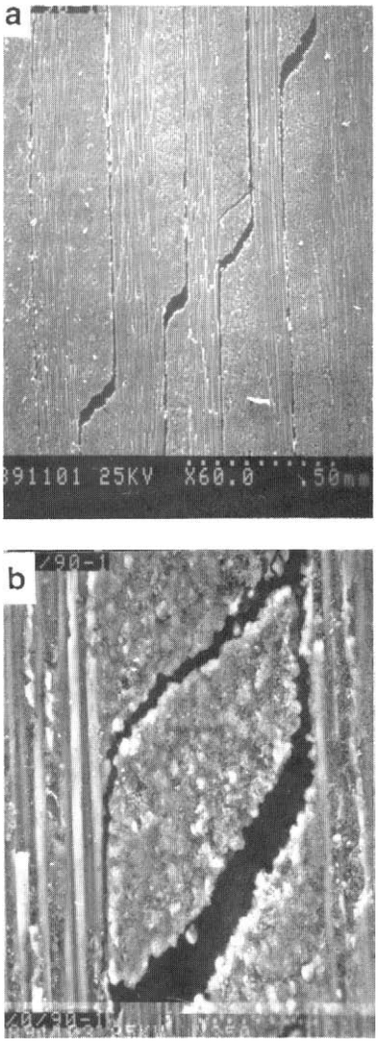

Figure 5 Mode II crack propagation in T300/MBMI $[0/90]_{6s}$ specimen

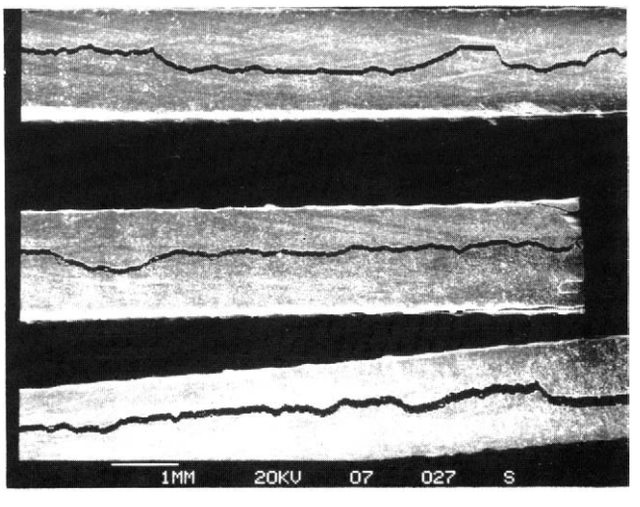

Figure 6 SEM micrograph showing mixed-mode delamination in three T300/MBMI $[\pm 30_2/90/\overline{90}]_s$ specimens

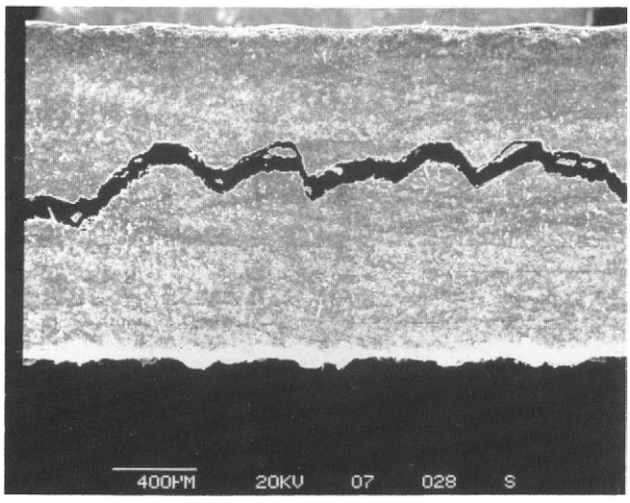

Figure 7 SEM micrograph showing that edge delamination occurs mainly at the $-30/90$ interface of T300/MBMI under mixed-mode loading

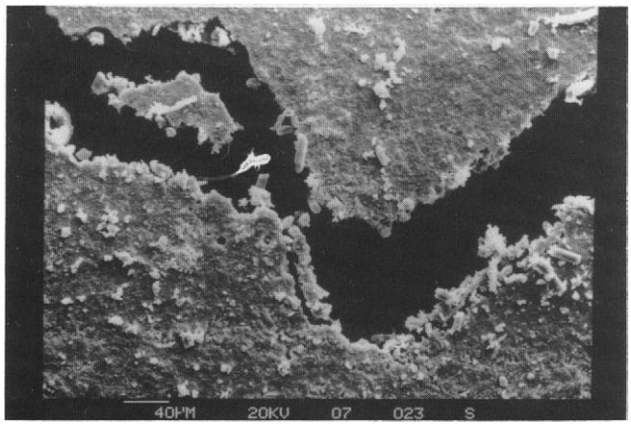

Figure 8 Edge delamination (high magnification) in T300/MBMI $[\pm 30_2/90/\overline{90}]_s$ under mixed-mode loading

TOUGHENING MECHANISMS OF CARBON/MBMI COMPOSITES

The interlaminar fracture toughnesses G_{Ic} and G_{IIc} of unidirectional T300/MBMI are higher than those of T300/epoxy composites by factors of 2 and 1.5, respectively. This reflects a significant toughening effect, which arises from the microstructure and properties of the modified bismaleimide matrix.

This new MBMI system is prepared by co-reacting oligomers of a bismaleimide and PES. Upon curing, a crosslinked polymer structure is formed which has excellent thermal and mechanical properties. The elongation at break is 2.2%, the fracture work is 2381 N m, and the tensile strength and modulus are 65.6 MPa and 3.5 GPa, respectively. The glass transition temperature (T_g) is 278°C. All of these values are substantially higher than those of conventional epoxy and other BMIs[7–9]. The transverse tensile strength σ_T and interlaminar shear strength τ_{ILSS} of T300/MBMI are higher than those of T300/epoxy by factors of 2 and 1.25, respectively[9]. This indicates that the adhesive strength and toughness of the

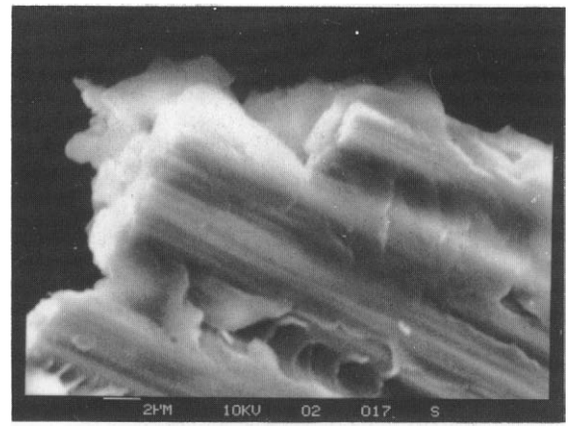

Figure 9 Interface state of T300/MBMI specimen under mixed-mode loading

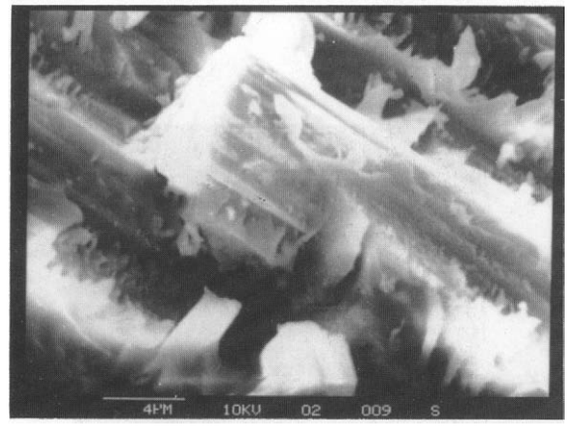

Figure 10 Interface state of T300/epoxy specimen under mixed-mode loading

T300 fibre/MBMI matrix interface are better than those of T300/epoxy.

SEM fractography also supports the above argument. The interface bonding of T300/MBMI (*Figures 9, 11*) is superior to that of T300/epoxy (*Figures 10, 12*) specimens. The MBMI matrix is uniformly adhered to the surfaces of the fibres, thereby providing adequate protection. As shown in *Figure 11*, some thermoplastic particles (size about 3 μm) of the matrix adhere to the fibres and shear bands are formed. Therefore there is more energy consumption when delamination occurs. The hackles of T300/MBMI are dense and irregular, but in the epoxy matrix the fracture surface is brittle and there are some resin-rich regions (*Figure 12*).

The presence of plastic deformation in MBMI leads to a delay in matrix cracking and interface debonding. As a result, the interlaminar fracture toughness becomes higher. Because plastic deformation is more extensive in the ENF specimens than in the DCB specimens, G_{IIc} is higher than G_{Ic}. From real-time bending failure fractography the delamination and transverse cracking of the ± 45 layers in the T300/epoxy laminate (*Figure 13*) are more serious than those in the T300/MBMI laminate (*Figure 14*). The interlaminar bonding in the T300/

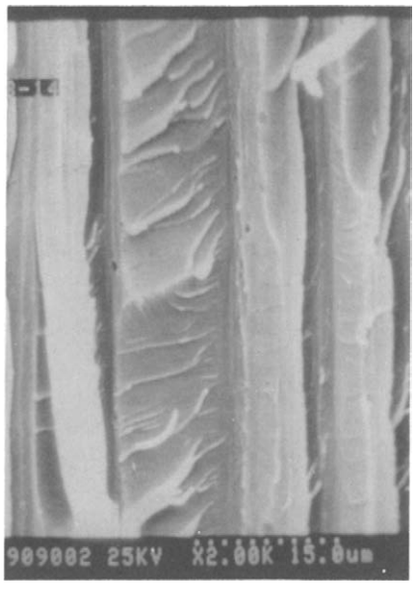

Figure 11 Fractograph showing shear hackles of T300/MBMI specimen

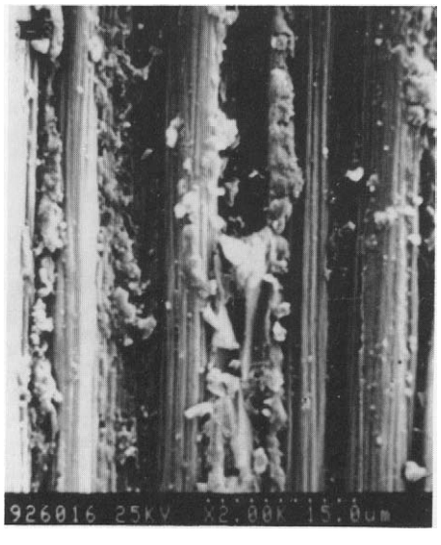

Figure 12 Brittle fracture surface and poor adhesion of T300/epoxy specimen

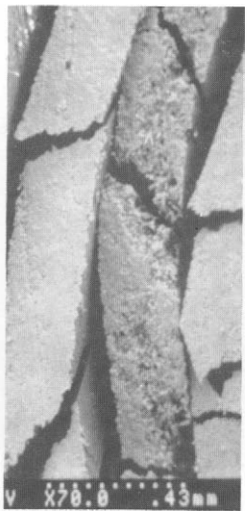

Figure 13 Dynamic bending failure of T300/epoxy $[\pm 45]_{6s}$ laminate under Mode II loading

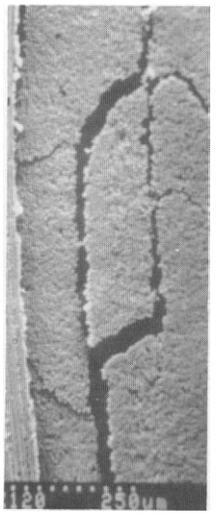

Figure 14 Dynamic bending failure of T300/MBMI $[\pm 45]_{6s}$ laminate under Mode II loading

MBMI laminate is rather strong and the transverse cracks are fine.

The primary cause of toughening is the presence of plastic deformation and various irregular shear hackles in the MBMI matrix. The secondary mechanism is a satisfactory interface adhesion. Both of these contribute to an increase in energy dissipation.

CONCLUSIONS

The interlaminar fracture toughnesses G_{Ic} and G_{IIc} of T300 carbon fibre-reinforced modified bismaleimide composites are higher than those of T300/epoxy composites by factors of 2 and 1.5, respectively. G_{mc} for the composite with BMI matrix is 70% higher.

This toughening effect results from an increase in matrix toughness and improvement in interface bonding. In MBMI composites, there is much more disorder in the arrangement and shape of the shear bands and hackles under loading, thereby leading to an increase in energy release when debonding occurs.

In general, the interlaminar fracture toughness of $[0]_{26}$ laminates is higher than those of $[0/90]_{6s}$ and $[\pm 45]_{6s}$ laminates, because there are fibres bridging the crack in the $[0]_{26}$ laminates. In multidirectional laminates, the delamination propagates mainly along the precrack direction but branching also occurs.

Interlaminar fracture studies in a scanning electron microscope allow the *in situ* observation and recording of the dynamic propagation of delamination and damage of fibre/matrix interface. This is an effective approach for elucidating the toughening mechanisms in composites with modified BMI matrix.

ACKNOWLEDGEMENTS

This work was supported by the Croucher Foundation of Hong Kong and the National Science Foundation of China. The authors wish to express their appreciation to Mr D.Y. Li and Mr G. Sheng for their assistance with the measurements.

REFERENCES

1 Whitney, J.M., Browning, C.E. and Hoogsteden, W.A. *J. Reinf. Plast. Compos.* 1982, **1**, 297
2 Gillespie, J.W., Carlesson, L.A. and Smily, A.J. *Compos. Sci. Technol.* 1987, **28**, 1
3 Salpekar, S.A. and O'Brien, T.K. in *ASTM STP 1110* (Ed. J.G. Williams, *et al.*), American Society for Testing and Materials, Philadelphia, PA, 1991, pp. 287–311
4 Friedrich, K. (Ed.) 'Application of Fracture Mechanics to Composite Materials', Elsevier Science Publishers BV, Amsterdam, 1989, pp. 82–154
5 Ramkumar, R.L. and Whitecomb, J.D. in *ASTM STP 876* (Ed. W.S. Johnson), American Society for Testing and Materials, Philadelphia, PA, 1985, pp. 315–335
6 Lefebvre, D. and Bathias, D.C. in 'Proc. ICCM-6' (Ed. F.L. Matthews), Elsevier, London, 1987, pp. 331 345
7 *Adv. Compos. Bull.*, 1989, **2**(9), 2
8 Byung, H., Lee, M., Ashraf, C. and Yefin, B. *Polym. News* 1988, **13**, 297
9 Zhao, Q.S., Li, Y.H., Cao, Z.H. and Sun, D.S. in 'Proc. 34th Int. SAMPE Conf.', SAMPE, Covina, CA, 1989, pp. 27–32
10 O'Brien, T.K. in *ASTM STP 775* (Ed. K.L. Reifsnider), American Society for Testing and Materials, Philadelphia, PA, 1982, pp. 140–167
11 Irwin, G.R. in 'Structural Mechanics', Pergamon Press, New York, 1960, pp. 557–591
12 Russell, A.J. and Street, K.N. in 'Progress in Science and Engineering of Composites, Proc. ICCM-IV' (Ed. T. Hayashi, K. Kawata and S. Omekawa), Japan Soc. Composite Mater., Tokyo, 1982, p. 279
13 Mall, S. and Johnson, W.S. *NASA-TM-86355*, National Aeronautics and Space Administration, Washington, DC, 1985
14 Sela, S. and Ishai, O. *Composites* 1989, **20**, 423